Received: 22 November 2023 | Accepted: 19 February 2024

DOI: 10.1002/biof.2051

RESEARCH ARTICLE

Biofactors WILEY

# Indicaxanthin prevents eryptosis induced by cigarette smoke extract by interfering with active Fas-mediated signaling

**Ignazio Restivo**[1] | **Ilenia Concetta Giardina**[1] | **Rosario Barone**[2] | **Antonio Cilla**[3] | **Stefano Burgio**[2] | **Mario Allegra**[1] | **Luisa Tesoriere**[1] | **Alessandro Attanzio**[1]

[1]Department of Biological, Chemical and Pharmaceutical Science and Technologies, Università degli Studi di Palermo, Palermo, Italy

[2]Department of Biomedicine, Neuroscience and Advanced Diagnostics, Section of Human Anatomy, Università di Palermo, Palermo, Italy

[3]Nutrition and Food Science Area, Faculty of Pharmacy and Food Sciences, University of Valencia, Burjassot, Valencia, Spain

**Correspondence**
Luisa Tesoriere, Department of Biological, Chemical and Pharmaceutical Science and Technologies, Università degli Studi di Palermo, Via Archirafi 28, 90123 Palermo, Italy.
Email: luisa.tesoriere@unipa.it

**Funding information**
Università degli Studi di Palermo

## Abstract

A physiological mechanism of programmed cell death called eryptosis occurs in aged or damaged red blood cells (RBCs). Dysregulated eryptosis contributes to abnormal microcirculation and prothrombotic risk. Cigarette smoke extract (CSE) induces a p38 MAPK-initiated, Fas-mediated eryptosis, activating the death-inducing signaling complex (DISC). Indicaxanthin (Ind) from cactus pear fruits, is a bioavailable dietary phytochemical in humans and it is able to incorporate into RBCs enhancing their defense against numerous stimuli. This in vitro work shows that Ind, at concentrations that mimic plasma concentrations after a fruit meal, protects erythrocytes from CSE-induced eryptosis. CSE from commercial cigarettes was prepared in aqueous solution using an impinger air sampler and nicotine content was determined. RBCs were treated with CSE for 3 h in the absence or presence of increasing concentrations of Ind (from 1 to 5 μM). Cytofluorimetric measurements indicated that Ind reduced CSE-induced phosphatidylserine externalization and ceramide formation in a concentration-dependent manner. Confocal microscopy visualization and coimmunoprecipitation experiments revealed that Ind prevented both CSE-triggered Fas aggregation and FasL/FADD/caspase 8 recruitment in the membrane, indicating inhibition of DISC assembly. Ind inhibited the phosphorylation of p38 MAPK, caspase-8/caspase-3 cleavage, and caspase-3 activity induced by CSE. Finally, Ind reduced CSE-induced ATP depletion and restored aminophospholipid translocase activity impaired by CSE treatment. In conclusion, Ind concentrations comparable to nutritionally relevant plasma concentrations, can prevent Fas-mediated RBC death signaling induced by CSE, which suggests that

**Abbreviations:** Ac-DEVD-pNA, *N*-acetyl-asp-glu-val-asp p-nitroanilide; APLT, aminophospholipid translocase; BSA, bovine serum albumin; CSE, cigarette smoke extract; DISC, death-inducing signaling complex; FADD, fas-associated via death-domain; FasL, Fas ligand; FITC, fluorescein isothiocyanate; HRP, horseradish peroxidase; Ind, Indicaxanthin; NBD-PS, nitrobenzoxadiazole-labeled phosphatidylserine; p-NA, p-nitroanilide; PS, phosphatidylserine; PVDF, polyvinylidene difluoride; RBCs, Red blood cells; TBS, tris-buffered saline; TBST, tris-buffered saline containing tween 20.

  

dietary intake of cactus pear fruits may limit the deleterious effects of cigarette smoking.

KEYWORDS
betalains, cell death, cigarette smoke, eryptosis, erythrocytes, indicaxanthin

## 1 | INTRODUCTION

Eryptosis is a programmed death mechanism that allows the removal of damaged red blood cells (RBCs) by phagocytes before natural senescence.[1] Long associated with pathologies such as metabolic syndrome,[2] acute cardiac insufficiency[3] and chronic kidney disease,[4] or with the intake of drugs and xenobiotics,[5] enhanced eryptosis has also recently been related to lifestyle habits as smoking status.[6] Because of the adhesiveness of the apoptotic RBCs to the vascular cells or platelets, excessive eryptosis induces an inflammatory response that can promote endothelial dysfunction, stimulate the formation of clots and compromise microcirculation under normal and pathological circumstances.[7,8]

Eryptosis shares several features with apoptosis, such as cell shrinkage, membrane blebbing, and membrane phospholipid scrambling with phosphatidylserine (PS) exposure at the cell surface.[9] However, as erythrocytes lack mitochondria, that are essential in the execution of the programmed cell death, the signaling leading to eryptosis is not identical to that underlying apoptosis. Mechanistically, triggers of eryptosis such as increase endocellular $Ca^{2+}$ ions, oxidative stress or energy depletion, lead to activation of proteases such as calpain or caspase 3, which are responsible for the cleavage of various membrane proteins causing cell membrane blebbing.[1,5] In addition, as a heritage of the erythroid maturation process, mature RBCs contain all the components of the extrinsic apoptotic pathway,[10] which can be activated in the presence of various stimuli. In vivo studies on animal models have demonstrated that chronic exposure to arsenic derivatives or lead induces Fas-activated erythrocytes death.[11,12] In humans, Fas-associated signaling complex has been detected in erythrocytes from cigarette smokers.[13]

A growing body of ex vivo and in vivo evidences point out that some natural products or phytochemicals, interfering with the biomolecular pathways that regulate the eryptosis machinery, can be effective in contrasting RBCs death.[14] Indicaxanthin (Ind) (Figure 1) is a betalain pigment of the edible fruits of *Opuntia ficus indica* (L. Mill) whose bioactivity has long been studied in our laboratory (for a recent review, see Reference 15). A number of investigations in cultured cell lines as well as in experimental animals indicate that Ind is a redox-active compound able to exert significant pharmacological effects ranging from the anti-inflammatory[16,17] to the neuro-modulatory[18] and anti-tumoral ones.[19] The molecular mechanism of the actions of this natural molecule is not yet fully elucidated. Ind's proven ability to modulate cell signaling pathways and gene expression may underlie its multiple effects. Interestingly, this dietary pigment is highly bioavailable in humans and attains a plasma peak of low micromolar concentration (6–7 μM) at 3 h from a fruit meal providing four fresh fruits.[20] Moreover, owing to its chemical–physical properties that allow it to interact with phospholipid bilayers,[21] Ind is able to incorporate in circulating RBCs offering antioxidative protection against various injuries.[22,23]

Toxicity of smoke components on isolated human RBCs has been recently studied in our laboratory. We demonstrated that cigarette smoke extract (CSE) induces eryptosis by p38 MAPK-initiated DISC formation followed by activation of caspase-8/caspase-3 via ceramide formation.[13] Given the bioactivity of Ind in RBCs and causative relationship linking cigarette smoke to eryptosis, in this in vitro work we investigated whether the pigment was able to interfere with the CSE-induced pathway of programmed cell death, preventing or mitigating the cytotoxic action of cigarette smoke on human erythrocytes. For this purpose, isolated RBCs were exposed to cigarette smoke products in the presence of Ind. Concentration from 1 to 5 μM was chosen while treating cells for 3 h considering the time interval during

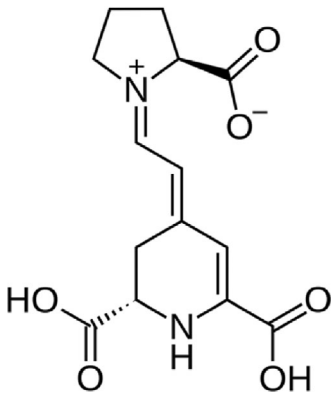


FIGURE 1 Molecular structure of Ind.

which the pigment gains these plasma concentrations and incorporates into circulating erythrocytes after a cactus pear fruit intake.[20,22] The CSE concentrations were in accordance to the previous study on the eryptotic action of cigarette smoke.[13]

## 2 | EXPERIMENTAL PROCEDURES

Unless specified, all chemicals were purchased from Merck Life Science (Milan, Italy) and were of the highest purity grade available.

### 2.1 | Extraction and purification of indicaxanthin

Ind was isolated from yellow fruits of *Opuntia ficus-indica* L. Mill by aqueous extraction. Purification was performed by size-exclusion chromatography on Sephadex G-25 column followed by reversed-phase semi-preparative high-performance liquid chromatography coupled with a UV/visible detector set at 482 nm as previously reported.[24] Aliquots containing the pigment were collected, submitted to cryo-desiccation and stored at −80°C until use. When required, samples were re-suspended in Ringer solution and Ind concentration was spectrophotometrically determined at 482 nm using a molar extinction coefficient of 42,800 $M^{-1}$ $cm^{-1}$.[25] After dilution at suitable concentration, Ind was filtered through a Millex HV 0.2 μm filter (Millipore, Billerica, MA, USA, Cat. No. SLHV033RS) immediately before use.

### 2.2 | Preparation of CSE

The smoke from three filtered cigarettes (Marlboro Red, Philip Morris USA Inc., Richmond, VA, USA) was directly absorbed in 30 mL of Ringer solution using an impinger air sampler, as previously reported.[13] This extract was considered as 100% CSE. Concentration of nicotine was assessed by LC–MS analysis.[13] Nicotine mean concentration of four different CSE preparations was 30.22 ± 1.84 mg/L.

### 2.3 | RBCs and treatment

Fresh blood samples were collected in heparinized tubes from healthy nonsmoking male volunteers ($n = 8$; age range 33–66 years; normal BMI range) with informed consent, and erythrocytes were isolated by centrifugation (2000*g*, 4°C, 20 min) on a Ficoll gradient (Sigma-Aldrich, Milan, Italy, Cat. No. F5415). Then RBCs were washed twice with Ringer's solution and diluted to 0.4% hematocrit with Ringer alone or Ringer containing 10% or 20% CSE, either in the absence or in presence of Ind. Samples were incubated in 24-multiwell for 3 h in humidified 5% $CO_2$ atmosphere at 37°C. The experimental study protocol was approved by the Ethic Committee of Palermo 1, University Hospital (No. 169/2023) and performed in accordance with the Declaration of Helsinki and its amendments.

### 2.4 | Measurement of PS externalization

Erythrocytes were washed twice in Ringer's solution, pH 7.4, and adjusted to $1.0 \times 10^6$ RBCs/mL with binding buffer following the manufacturer's instructions. One hundred microliters of cell suspension were incubated with 5 μL of Annexin V-fluorescein isothiocyanate (FITC) (eBioscience, San Diego, CA, USA, Cat. No. 88-8005-74) at room temperature in the dark for 15 min. Then, suspension samples were subjected to flow cytometric analysis with Epics XL™, using the Expo32 software (Beckman Coulter, Fullerton, CA). At least $1 \times 10^4$ events were analyzed for each sample using ungated images.

### 2.5 | Measurement of ceramide

After treatment, $1.0 \times 10^5$ RBCs were incubated for 1 h at 37°C with 1 μg/mL of mouse monoclonal anti-ceramide antibody (Sigma-Aldrich, Cat. No. C8104) in PBS containing 0.1% bovine serum albumin (BSA). After two washing steps with PBS-BSA to remove unbound antibody, RBCs were incubated for 30 min with 20 μL of a goat anti-mouse, polyclonal, FITC-conjugated, secondary antibody (Millipore, Billerica, MA, USA, Cat. No. AQ502F) diluted 1/50 in PBS-BSA in the dark. Finally, erythrocytes were collected by centrifugation (2000*g*, 4°C, 5 min), washed twice, resuspended in PBS and analyzed by flow cytometer. For each sample, at least $10^4$ events were analyzed as above reported, using ungated images.

### 2.6 | Immunoprecipitation

RBCs ($2.0 \times 10^8$ cells) were washed twice with PBS, resuspended in lysis buffer (20 mM Tris–HCl, pH 7.6, 100 mM NaCl, 10 mM $MgCl_2$, 1% NP-40, 2 mM PMSF, 0.5 mM DTT and 2 mg/mL lysozyme) containing phosphatase (Roche, Basel, Switzerland, Cat. No. 4906845001)

and protease inhibitors (Roche, Cat. No. 4693132001). Subsequently, the cells were lysed by two cycles of sonication (each in ice for 30 sec with Labsonic LBS1-10, Treviglio, Italy). After centrifugation (40,000*g*, 4°C for 1 h), supernatants were immunoprecipitated overnight with mouse anti-FAS antibody (1:200) (Santa Cruz, Biotechnology, Dallas, TX, USA, sc-74540) at 4°C and then incubated with 20 μL of Protein G PLUS-Agarose (sc-2002) for 3 h at 4°C. The pellets were washed twice in lysis buffer and proteins were separated by SDS-PAGE for immunodetection by western blotting.

## 2.7 | Western blotting

Proteins contained in supernatants from lysated RBCs ($2.0 \times 10^8$ cells) were quantified by Bradford (Bio-Rad, Hercules, CA, USA, Cat. No. 5000006). Equal quantities of proteins (50 μg/lane) for each sample were separated by discontinuous 10% SDS-PAGE and electrotransferred onto a polyvinylidene difluoride (PVDF) membrane (Millipore, Cat. No. IPVH00010). Blots were treated with blocking solution (5% nonfat dry milk) and then incubated overnight at 4°C with primary antibodies in Tris-buffered saline (TBS; 25 mM Tris, 150 mM NaCl, pH 7.4) containing Tween 20 (1%, v/v) (TBST) and 5% (w/v) BSA. Mouse monoclonal anti-FADD (sc-271,748), anti-Fas (sc-74,540), anti-FasL (sc-33716), anti-caspase-3 (sc-56053), anti-caspase-8 (sc-81657), anti-p-p38 MAPK (sc-166182), anti-p38 MAPK (sc-7972), and anti-Actin (sc-8432) were used at a dilution of 1:200. After washing three times with TBST, membranes were incubated with a 1:2000 dilution of the secondary rabbit anti-mouse IgG antibody, horseradish peroxidase (HRP) conjugated (Sigma-Aldrich, Cat. No. AP160P) for 1 h at room temperature. Immunoblots were then washed six times with TBST and detected by enhanced chemiluminescence (Amersham, Milan, Italy, Cat. No. RPN2232). Densitometric analysis of protein spots was carried out using Quantity One Imaging Software (Bio-Rad, Cat. No. 1708265) and the results were reported as arbitrary densitometric units normalized to actin, Fas or p38 MAPK.

## 2.8 | Confocal microscopy

RBCs were fixed in methanol for 30 min on glass slides. Cells were incubated in the antigen unmasking solution (10 mM tri-sodium citrate, 0.05% Tween-20) for 8 min at room temperature and treated with a blocking solution (3% BSA in PBS) for 30 min. Then, primary antibodies were applied (Rabbit polyclonal anti-caspase-8, Cat. No. 13423-1-AP, Proteintech and Mouse monoclonal anti-Fas sc-74540), and the slides were incubated in a humidified chamber overnight at 4°C. The day after, the cells were incubated with a species-specific fluorescent secondary antibody conjugated, anti-rabbit IgG-Atto 647N (Sigma-Aldrich, Cat. No. 40839) and anti-mouse IgG-Atto 488 (Sigma-Aldrich, Cat. No. 62197), respectively, both diluted to 1:150. Finally, the slides were covered with drops of PBS and mounted with coverslips. Images were captured using a 63× objective in a Leica Confocal Microscope TCS SP8 (Leica Microsystems, Wetzlar, Germany).

## 2.9 | Caspase 3 activity

Activity of Caspase 3 was measured according to the of manufacturer's protocol (Millipore APT165—Caspase-3 Colorimetric Activity Assay Kit). This colorimetric assay is based on the hydrolysis of the peptide substrate *N*-Acetyl-Asp-Glu-Val-Asp p-nitroanilide (Ac-DEVD-pNA) to *p*-nitroanilide (p-NA) (absorbance at 405 nm). Briefly, after treatments, $2 \times 10^6$ RBCs were centrifuged and the pellet was homogenized in 200 μL of cold cell lysis buffer. The samples were subjected to 3 freezing/thawing cycles and then centrifuged at 13,000*g* for 2 min. Reaction mix was prepared in ice as follows: 50 μL of sample, 20 μL of $H_2O$, 20 μL of Assay Buffer 5X and 10 μL of Caspase Substrate 3 (Ac-DEVD-pNA). Mixture was incubated in 96-multiwell at 37°C for 120 min in the dark. Spectrophotometric analysis of p-NA was performed using a GloMax® Plate Reader (Promega™, Milan, Italy) and the amount was calculated by interpolation with the calibration curve of the p-NA standard.

## 2.10 | Determination of ATP

ATP level was measured according to the Abcam protocol (Cambridge, UK, Cat. No. ab83355—ATP Assay Kit). RBCs ($1 \times 10^7$ cells) were centrifuged, homogenized in 100 μL ATP assay buffer and frozen/thawed three times. Samples were then centrifuged at 13,000*g* for 2 min and supernatants were deproteinized in ice according to Abcam kit (ab204708—Deproteinizing Sample Preparation Kit—TCA). Reaction mix was prepared as follows: 50 μL sample, 46 μL assay buffer, 2 μL ATP converter and 2 μL developer mix. Reaction mixture has been incubated in 96-multiwell at 37°C for 30 min in the dark. ATP concentration was determined fluorometrically (GloMax® Plate Reader) at 535 nm excitation and 587 nm emission by interpolation with the calibration curve of the ATP standard.

## 2.11 | Aminophospholipid translocase (APLT) activity

APLT activity was measured using flow cytometry by translocation of labeled phospholipid from the outer to the inner membrane leaflet, as described by Tesoriere et al.[26] Briefly, RBC suspensions ($2 \times 10^7$ cells) were incubated at 37°C with 0.5 mM nitrobenzoxadiazole-labeled PS (NBD-PS) fluorescent probe (Avanti Polar Lipids, Alabaster, AL, USA), added from a 1 mmol/L stock solution in HEPES-buffer. After 60 min, 5 μL of the sample was added to 250 μL HEPES buffer containing 0.1 mM EGTA and 1% BSA, that extracts only surface-associated NBD-PS probe. Cytofluorimetric analysis of residual fluorescence of the sample reveals the amount of NBD-PS localized in the inner leaflet of the plasma membrane as result of the APLT activity. For each sample, at least $10^4$ events were analyzed.

## 2.12 | Statistical analysis

Results are expressed as mean ± SD of ($n$) independent experiments carried out in triplicates. Statistical comparisons were performed by one-way analysis of variance (ANOVA) followed by Tukey's correction for multiple comparisons using Prism 8.4 (GraphPad Software Inc., San Diego, CA, USA). A value of $p < 0.05$ was considered statistically significant.

# 3 | RESULTS

## 3.1 | Indicaxanthin inhibits CSE-induced eryptosis

Isolated human RBCs were exposed for 3 h to either 10% or 20% CSE in the absence or in the presence of 1 to 5 μM Ind. As shown in Figure 2, CSE increased two of the major hallmarks of eryptosis, that is, PS externalization on membrane outer leaflet (A) and ceramide formation (B), measured by flow cytometry by annexin V-FITC staining and labeled secondary antibody, respectively. Ind, in a concentration dependent manner, reduced the CSE-induced increase of both annexin V-binding fluorescent cells (Figure 2A) and ceramide levels (Figure 2B) under each treatment condition. In 10% CSE-exposed RBCs, Ind at 5 μM inhibited the PS externalization and the ceramide production by 75% and 80%, respectively. The protective effect of 5 μM Ind in RBCs treated with

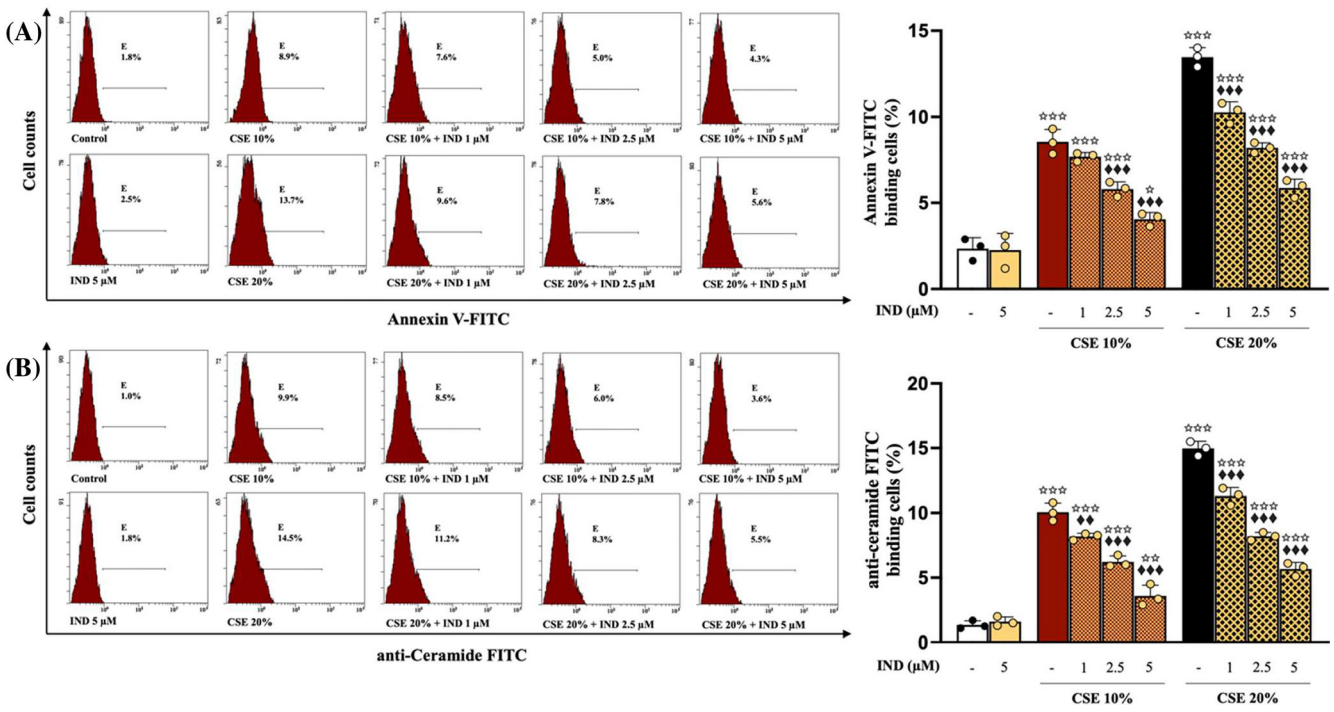


FIGURE 2 Indicaxanthin inhibits PS exposure and ceramide production in CSE-induced eryptosis. (A) Percentage of PS-exposing erythrocytes and (B) ceramide levels in RBCs exposed for 3 h to vehicle or CSE in the absence or in the presence of Ind. Levels of annexin-V binding cells and ceramide were measured by flow cytometry as reported at Sections 2.4 and 2.5 of experimental procedures. Values are means ± SD of three independent experiments carried out in triplicate. ☆$p < 0.05$, ☆☆☆$p < 0.001$ versus control; ◆◆$p < 0.01$, ◆◆◆$p < 0.001$ versus relevant treatment with CSE.

20% CSE was slightly weaker, with an inhibition of PS externalization and ceramide formation by about 67% and 65%, respectively. No appreciable effect of Ind was evident in the absence of CSE (Figure 2).

### 3.2 | Indixanthin inhibits the CSE-induced assembly of the death-inducing signaling complex (DISC)

The effect of 5 μM Ind on the recruitment in membrane of Fas ligand (FasL), Fas-associated via death-domain (FADD) and caspase 8, after treatment with CSE, was investigated by immunoprecipitation technique with anti-Fas, followed by western blotting of the *immunoprecipitate* with proper antibody. Densitometric analysis of the blots showed that Ind reduced the amounts of each protein component of DISC in the *immunoprecipitates* from the CSE-treated RBCs (Figure 3). In comparison with RBCs treated with 10% CSE alone, Ind prevented the recruitment in membrane of FADD and caspase 8 and reduced the amount of FasL by about 80%. The inhibition of DISC formation in RBCs treated with 20% CSE was weaker than that in the cells exposed to 10% CSE. Indeed, in comparison with RBCs treated with 20% CSE alone, Ind inhibited the membrane recruitment of

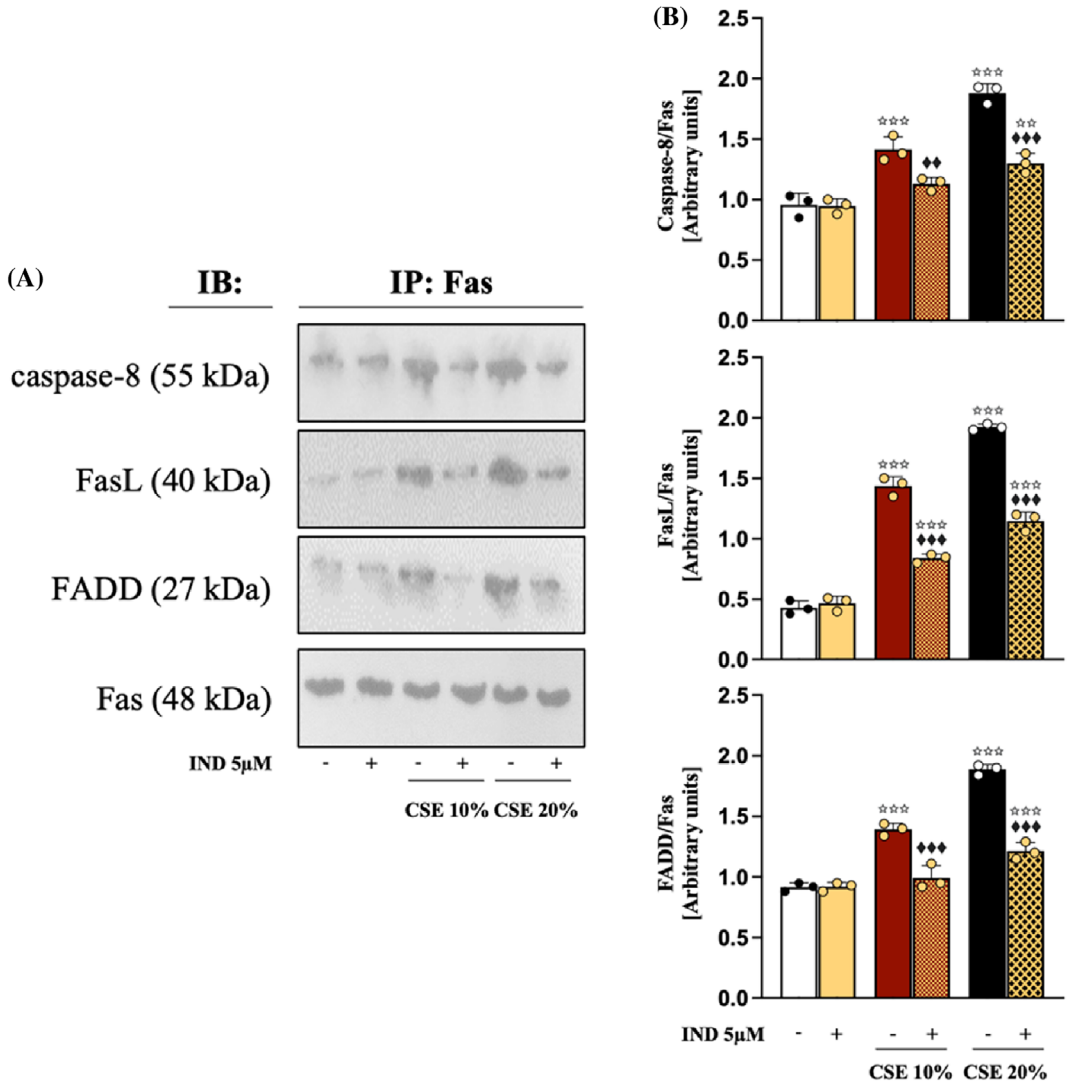


**FIGURE 3** Indicaxanthin inhibits CSE-induced DISC assembly. (A) Representative images of immunodetections of caspase-8, FasL, and FADD after immunoprecipitation with anti-Fas antibody in RBCs exposed for 3 h to vehicle or CSE in the absence or in the presence of Ind. Blots were reprobed with anti-Fas antibody to ensure equal loading of the gels. (B) Densitometric analysis of caspase-8, FasL, and FADD levels normalized for Fas. Immunoprecipitation, SDS-PAGE, and immunodetection of the proteins were as reported at Sections 2.6 and 2.7 of experimental procedures. Values are the means ± SD of bands' densitometry of three independent experiments with comparable results. ☆☆$p < 0.01$, ☆☆☆$p < 0.001$ versus control; ◆◆$p < 0.01$, ◆◆◆$p < 0.001$ versus relevant treatment with CSE.

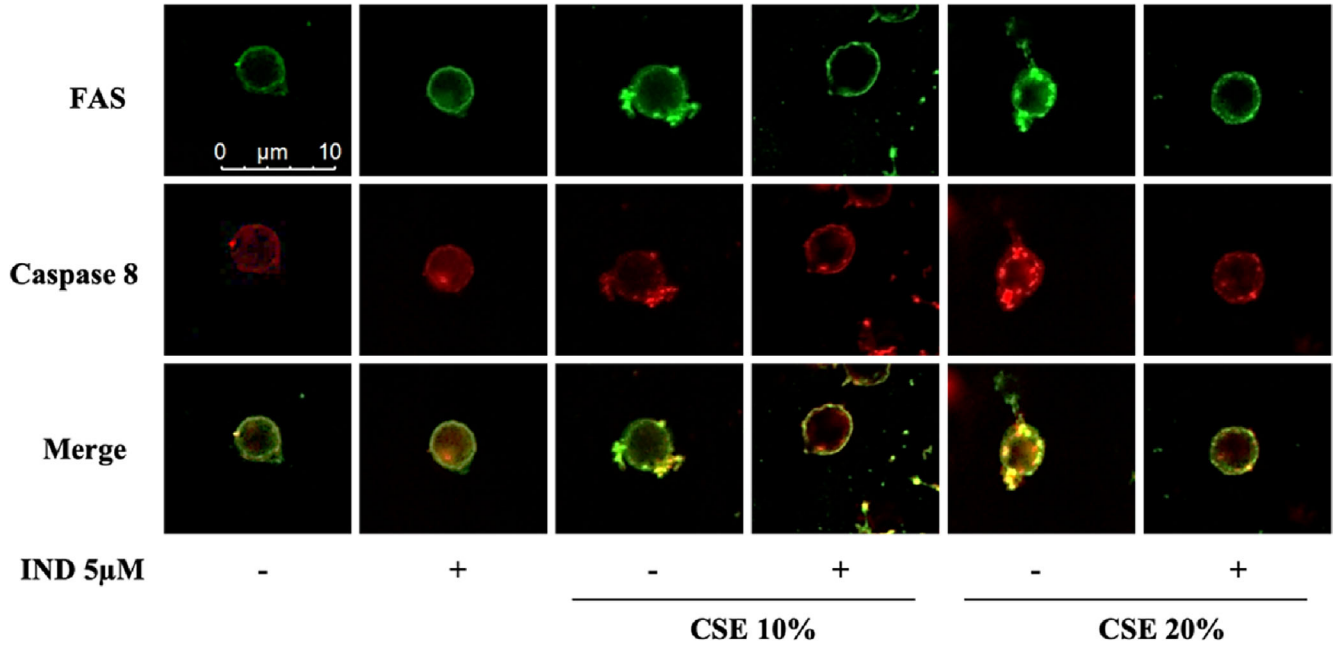


**FIGURE 4** Indicaxanthin inhibits the CSE-induced association of Fas with caspase-8 in RBCs membrane as demonstrated by confocale microscopy. RBCs were exposed for 3 h to vehicle or CSE in the absence or in the presence of Ind. Cells were fixed in methanol and labeled for immunofluorescent detection of Fas and caspase-8 as reported in Section 2.8 of experimental procedures. The images were captured using a Leica Confocal Microscope TCS SP8 (Leica Microsystems) bar = 10 µm for all panels. Colocalization of Fas with caspase-8 was revealed upon merging. Representative images of two independent experiments.

FasL, FADD and caspase 8 by 53%, 69%, and 63%, respectively.

Single-cell image study with confocal microscopy was performed to confirm the CSE-induced association of Fas death receptor with caspase 8 and the inhibition of Ind. In untreated RBCs, immunolabeling of Fas indicated the presence of the receptor spread in the plasma membrane, whereas caspase-8 appeared dispersed in the cytosol (Figure 4). No significantly different immunofluorescence images were evident in the presence of Ind only. On the contrary, treatment of the cells with CSE at either 10% or 20% caused aggregation of Fas in localized patches and translocation of caspase 8 to the membrane. Merging of the images suggested that caspase 8 co-localized with Fas in plasmamembrane (Figure 4). Ind inhibited both Fas clustering and association with caspase-8 under both CSE treatment conditions (Figure 4).

### 3.3 | Indicaxanthin inhibits CSE-induced p38 MAPK and caspase-8/caspase 3 activation

CSE-induced DISC formation in erythrocytes is controlled by p38-MAPK.[13] In our study, immunoblotting analysis of cell lysates of RBCs exposed for 3 h at 10% or 20% CSE showed an increment of active p-p38/ inactive p38 MAPK ratio (∼3-fold and ∼4-fold, respectively) (Figure 5). Ind 5 µM totally inhibited the phosphorylation-mediated activation of p-38 MAPK caused by treatment with 10% CSE, while it reduced p-p38 MAPK levels by 75% in favor of the inactive unphosphorylated form when RBCs were exposed to 20% CSE (Figure 5).

CSE-induced DISC assembly triggers the proteolytic autoactivation of caspase-8, which in turn activates downstream caspase-3 by cleavage.[13] Under our experimental conditions, a 10- and 20-fold increase in the appearance of both active caspase-8 p18 subunit and active caspase-3 p17 subunit was observed by immunoblotting in RBC treated with 10% or 20% CSE, respectively (Figure 5). Relevantly, co-incubation with 5 µM Ind resulted in an 80% reduction of the cleaved procaspase 8 measured after both treatments, while it produced a weaker inhibition on the formation of the active 17 kDa fragment of caspase-3 (64% and 76% inhibition in 10% or 20% CSE treated RBCs, respectively) (Figure 5).

Next, we tested the functional activation of caspase-3 in the CSE-mediated eryptosis and the effect of Ind. As shown in Figure 6, exposure of RBCs to either 10% or 20% CSE for 3 h led to a dose-dependent activation of caspase-3, whose activity was determined by measuring the cleavage of the substrate Ac-DEVD-pNA. Co-incubation of the cells with the phytochemical at 5 µM resulted in a 60% reduction of the CSE-stimulated

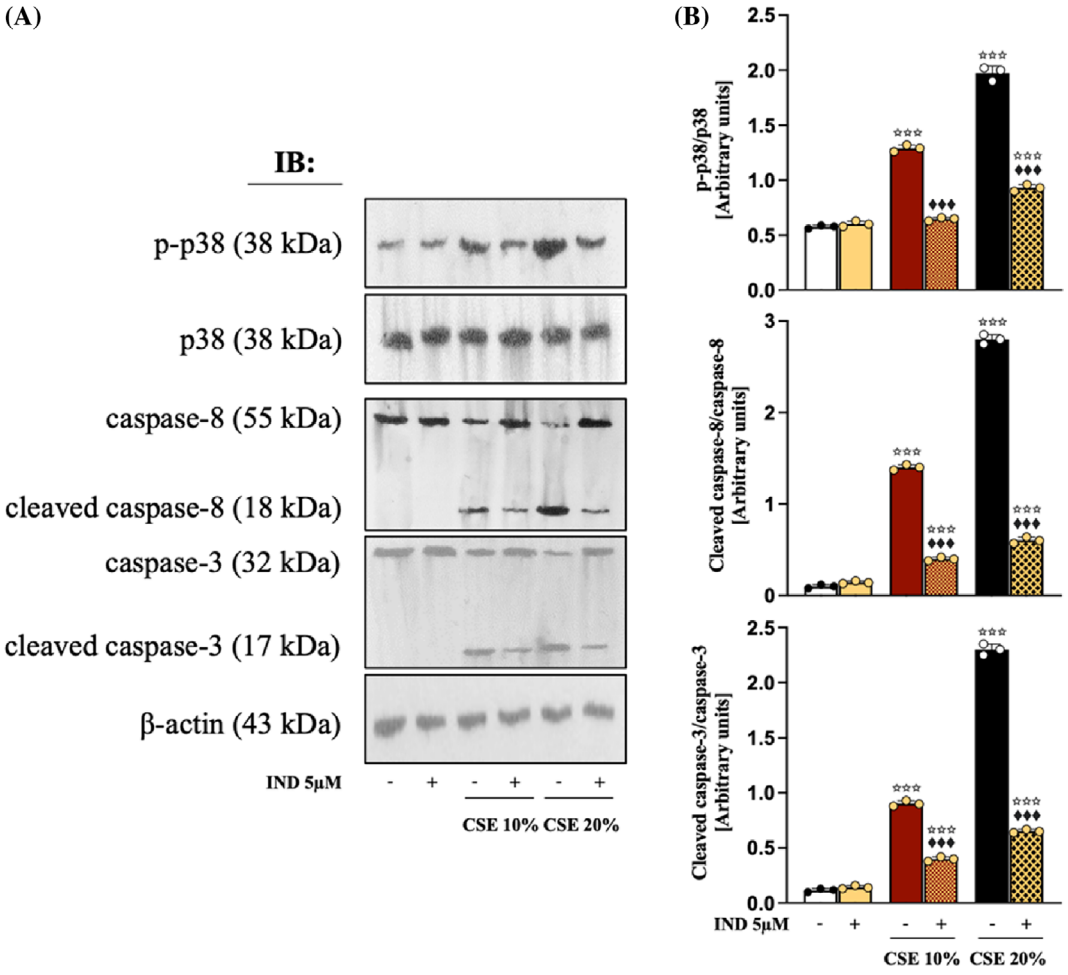


**FIGURE 5** Indicaxanthin inhibits p38 MAPK phosphorylation and caspase-8/3 cleavage in CSE-induced eryptosis. (A) Representative images of immunodetections of p-38 MAPK, p-p38 MAPK and caspase-8/3 in RBCs exposed for 3 h to vehicle or CSE in the absence or in the presence of Ind. Blots were reprobed with anti-β-actin antibody to ensure equal loading of the gels. (B) Densitometric analysis of ratios between p-p38/p-38 MAPK and cleaved and uncleaved forms of caspase-8/3 normalized for β-actin. SDS-PAGE and immunodetection of the proteins were as reported at Section 2.7 of experimental procedures. Values are the means ± SD of bands' densitometry of three independent experiments with comparable results. ☆☆☆$p < 0.001$ versus control; ♦♦♦$p < 0.001$ versus respective treatment with CSE.

enzyme activity under each CSE treatment. The reliability of the substrate Ac-DEVD-pNA was checked preincubating RBCs with caspase 3 inhibitor Z-DEVD-FMK (100 μM) before exposure of the cells to CSE. In this condition, pNA release was not evident (Figure 6).

## 3.4 | Indicaxanthin inhibits CSE-induced ATP depletion and impairment of APLT activity

Energy depletion, ATP decrement and impairment of the membrane APLT have been associated to eryptotic process.[1,5,26] We investigated if CSE treatment affected the ATP levels in RBCs and the effect of Ind. In comparison to control RBCs, ATP concentration in erythrocytes treated with 20% CSE for 3 h was almost halved (1.37 ± 0.12 vs. 0.79 ± 0.04 μg/1 × $10^6$cells). We also preincubated RBCs with Z-DEVD-FMK before CSE treatment. As the caspase-3 inhibitor did not produce any significant recovery of the CSE-induced ATP depletion (Figure 7), can be concluded that impairment of cell energy metabolism is independent of the executive phase of death triggered by CSE, at least in the early phase of stimulation. When RBCs were exposed to CSE in the presence of 5 μM Ind, the ATP concentration was strongly preserved, amounting to about 85% of the control value (Figure 7).

Decrease of ATP may affect the membrane APLT activity, a flippase that transports PS from the outer to the inner leaflet of the plasma membrane against the concentration gradient. Inhibition of APLT results in loss of membrane PS asymmetry with exposure of the phospholipid at the cell surface. We assessed the APLT activity in RBCs exposed to CSE and the effect of Ind by flow

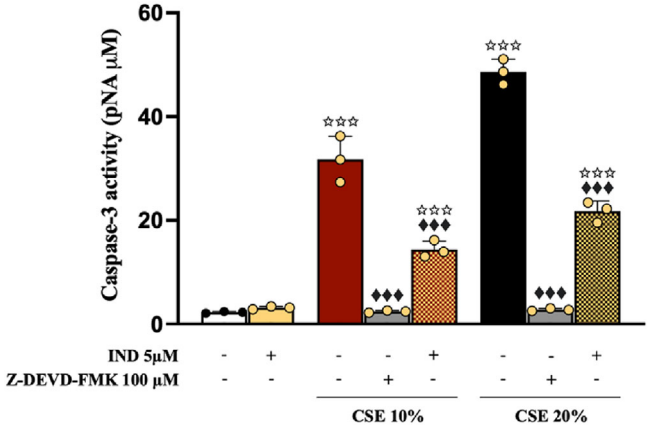


**FIGURE 6** Indicaxanthin inhibits CSE-induced caspase-3 activity. RBCs were exposed for 3 h to CSE or vehicle in the absence or in the presence of Ind or Z-DEVD-FMK. Caspase-3 activity was measured as reported in Section 2.9 of experimental procedures. Values are means ± SD of three independent experiments carried out in triplicate. ☆☆☆$p < 0.001$ versus control; ♦♦♦$p < 0.001$ versus respective treatment with CSE.

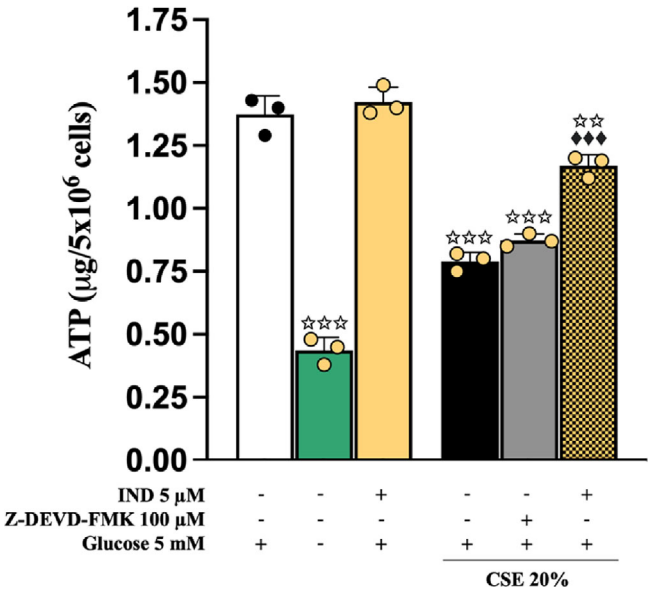


**FIGURE 7** Indicaxanthin inhibits CSE-induced ATP depletion. RBCs were exposed for 3 h to CSE or vehicle or Z-DEVD-FMK in the absence or in the presence of Ind. Levels of intracellular ATP were fluorometrically measured as reported in Section 2.10 of experimental procedures. As negative control, cells were incubated in RINGER lacking 5 mM glucose. Values are means ± SD of three independent experiments carried out in triplicate. ☆☆ $p < 0.01$, ☆☆☆$p < 0.001$ versus control; ♦♦♦$p < 0.001$ versus respective treatment with CSE.

cytometry by determining the percent of fluorescent-labeled phosphatidylserine (NBD-PS) translocated from the outer to the inner membrane leaflet. Therefore, NBD-PS negative cells are cells in which the flippase is inhibited. In comparison to control RBC, 3 h treatment of the cells with 20% CSE caused a 20% decrement of NBD-PS-associated cell fluorescence, while a smaller decrease (about 9%) was measured when 5 μM Ind was added (Figure 8).

## 4 | DISCUSSION

Plant foods not only provide nutrients but also secondary metabolites that can act as beneficial biofactors for health by positively influencing a range of biological functions through a variety of mechanisms. Ind, the yellow pigment of cactus pear fruit, possesses high intestinal absorption[20] and, after dietary intake, reaches peak concentration in plasma within 3 h of eating the fruit and can be distributed into circulating erythrocytes.[20,22] In the present study, using appropriate experimental timeframes and setting plasma concentrations of nutritional relevance, we show that the pigment protects human RBCs from toxic damage by cigarette smoke. Delving into the molecular mechanism of its protective effect, we provide evidence that Ind prevents the p38 MAPK-dependent Fas-activated extrinsic signaling pathway that leads the cells to eryptosis.

Aqueous CSE is one of various derivatives commonly used to test cytotoxicity of cigarette smoke in cell experiments. In human RBCs, we have recently reported that CSE triggers oxidative stress-independent eryptosis and induces DISC formation followed by activation of caspases-8/caspase-3.[13] By confocal microscopy visualization and coimmunoprecipitation experiments, we here demonstrate that Ind significantly reduces the CSE-induced PS externalization and prevents both Fas aggregation and FasL/FADD/caspase 8 recruitment in membrane. Overall Ind appears to inhibit the CSE-stimulated formation of DISC, the protein machinery involved in caspase-8 activation. Indeed, we also show that, when RBCs were exposed to CSE in the presence of the phytochemical, the uncleaved inactive form of caspase-8 prevails on the cleaved active one.

The CSE-activated extrinsic pathway of eryptosis includes formation of ceramide, a key lipid messenger in the Fas-dependent death-signaling,[27] and culminates in the activation of the executioner caspase-3.[13] We show that co-treatment of RBCs with Ind not only reduces the amount of ceramide induced by CSE, but also the amount of the cleaved caspase 3, resulting in inhibition of the enzyme's activity and blockage of the final phase of eryptosis.

p38 MAPK is a prominent mediator of the cellular stress response and its activation is required to start Fas-mediated eryptosis stimulated by CSE.[13] Various natural

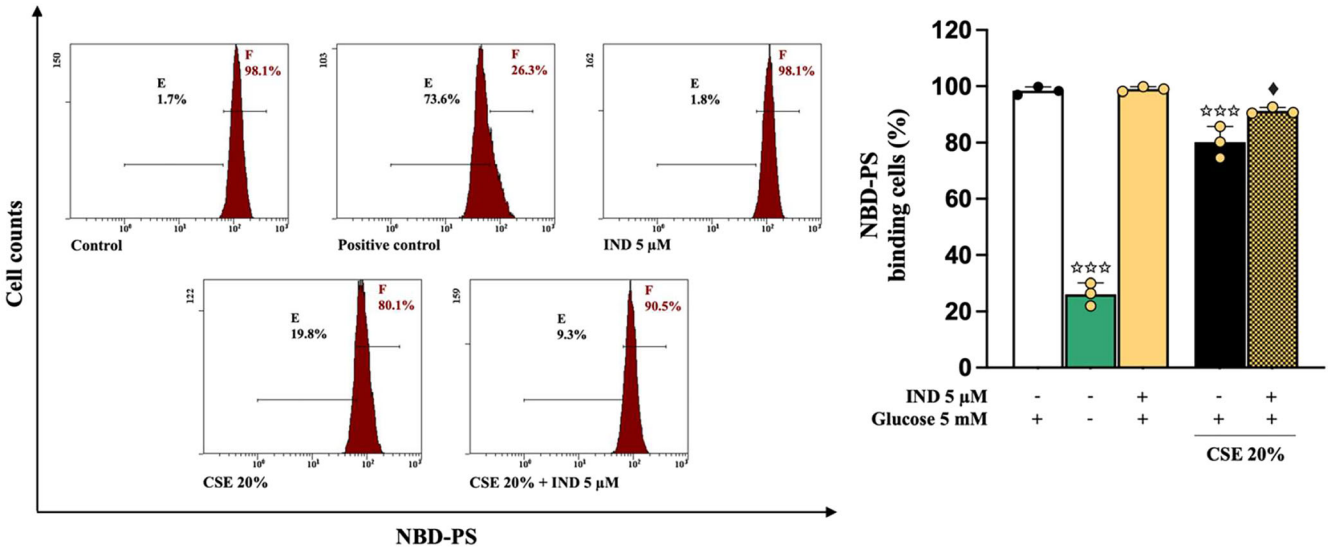


**FIGURE 8** Indicaxanthin prevents the CSE-induced APLT activity inhibition. RBCs were exposed for 3 h to CSE or vehicle in the absence or in the presence of Ind. Fluorescent-labeled PS (NBD-PS) translocated from the outer to the inner membrane bilayer was measured by flow cytometry as reported at Section 2.11 of experimental procedures. As negative control, cells were pre and incubated in RINGER lacking 5 mM glucose. Values are means ± SD of three independent experiments carried out in triplicate. ☆☆☆$p < 0.001$ versus control; ♦$p < 0.05$ versus respective treatment with CSE.

dietary compounds, such as polyphenols, have been observed to interfere with MAPKs activation mechanisms,[28] but the influence of Ind on members of the family of signaling proteins that mediate apoptosis is unknown. In the present study, immunoblotting experiments show that Ind inhibits CSE-induced phosphorylation of p38 MAPK, preventing activation of a major initiator of eryptosis.

We have previously reported that CSE-induced eryptosis does not involve either $Ca^{2+}$ entry or increase of cytosolic $Ca^{2+}$ activity.[13] Although this data allowed us to exclude involvement of scramblase in the externalization of the PS, the mechanism responsible for the loss of the membrane phospholipid asymmetry had remained undetermined. The data presented here provide new information. We show that CSE treatment reduces ATP levels and causes loss of the activity of APLT, an ATP-dependent flippase moving PS from the outer to the inner leaflet of the plasma membrane. In this scenario, we also demonstrate that Ind prevents the ATP depletion induced by CSE and restores the APLT activity. Taken together, these results indicate that, while blocking the initial phase of Fas-dependent eryptotic activity of CSE, namely p-38 MAPK activation, DISC assembly and caspase activation, Ind also protects the energy reserve of RBCs and contributes to the maintenance of PS in the inner leaflet of erythrocyte membrane.

Although the present data highlighted some novel mechanistic aspects of the eryptotic action of CSE and underlined the protective effect of Ind, it is worth emphasizing that other aspects of both processes remain elusive and deserve further investigation. Fall in cellular ATP levels has been reported by many authors, and by us, in association with the eryptotic fate of RBCs, however it has not yet been ascertained which event(s) contribute to fall in ATP. Impairment of glucose entry and/or metabolic fate, as well as a leakage of ATP from RBCs could be considered,[29] depending on the nature of the eryptotic trigger. In this framework, since we show that ATP depletion induced by CSE appears to be independent of caspase-3 activation, a possible protective action of Ind at level of glucose entry remains to be ascertained. In addition, molecular mechanisms through which Ind interferes with the CSE- induced eryptosis await to be depicted. Anti-apoptotic effects of Ind have previously been demonstrated in many cell models, including RBCs, in which cytotoxicity was induced by oxidative stress.[23,24] Since Ind is a redox-active molecule, its positive influence on redox-regulated signaling pathways involved in cell survival has been postulated.[15] The present study shows for the first time the ability of Ind to interfere with the Fas-activated, oxidative stress-independent cell death pathway. In such a process, the dynamic organization of membrane microdomains plays a crucial role in the initiation and transmission of receptor-mediated death signals. Ind, by virtue of its amphipatic moieties and its ability to partition within membrane phospholipids,[21] may be active in influencing membrane organization and modulating fluidity and the related survival molecular events. Along these lines,

evaluation of the ability of Ind to alter lipid raft arrangement is currently under study in our laboratory.

Cigarette smoking is a known risk factor for human health that contributes to the onset and progression of cardiovascular diseases, responsible for tens of millions of deaths per year.[30] Consequently, less expensive interventional strategies for preventing CS-related diseases, such as optimal dietary styles, could have positive repercussions on health systems management. Smokers have higher levels of circulating eryptotic RBCs than nonsmokers and excessive eryptosis contributes to vascular dysfunction.[6,31] In demonstrating that concentrations of Ind comparable with the nutritionally relevant plasma concentrations, can counteract the cigarette smoke-induced death of RBCs, our findings suggest that dietary intake of cactus pear fruits may restrict the deleterious effects of cigarette smoke in humans. Ind-enriched cactus pear fruit extracts could be developed and investigated as dietary integrators to overcome the seasonality of the fruit.

## AUTHOR CONTRIBUTIONS

*Conceptualization*: L.T. and I.R. *Methodology*: L.T., I.R., and A.A. *Software*: I.R. and I.C.G. *Validation*: L.T., I.R., and M.A. *Formal analysis*: I.R., A.A., and A.C. *Investigation*: A.A., I.R., I.C.G, R.B., and S.-B. *Resources*: L.T. *Data curation*: I.R. *Writing—original draft preparation*: L.T. and M.A. *Writing—review and editing*: L.T. and M.A. *Visualization*: A.A., I.C.G., and A.-C. *Funding acquisition*: I.R. All authors have read and agreed to the published version of the manuscript.

## ORCID

*Ignazio Restivo* https://orcid.org/0000-0003-1833-2356
*Luisa Tesoriere* https://orcid.org/0000-0002-7980-7530

## REFERENCES

1. Alghareeb SA, Alfhili MA, Fatima S. Molecular mechanisms and pathophysiological significance of eryptosis. Int J Mol Sci. 2023;24:5079.
2. Restivo I, Attanzio A, Tesoriere L, Allegra M. Suicidal erythrocyte death in metabolic syndrome. Antioxidants. 2021; 10(2):154.
3. Attanasio P, Bissinger R, Haverkamp W, Pieske B, Wutzler A, Lang F. Enhanced suicidal erythrocyte death in acute cardiac failure. Eur J Clin Invest. 2015;45(12):1316–24.
4. Lang F, Bissinger R, Abed M, Artunc F. Eryptosis—the neglected cause of anemia in end stage renal disease. Kidney Blood Press Res. 2017;42:749–60.
5. Lang F, Lang E, Föller M. Physiology and pathophysiology of eryptosis. Transfus Med Hemother. 2012;39:308–14.
6. Attanzio A, Frazzitta A, Vasto S, Tesoriere L, Pintaudi AM, Livrea MA, et al. Increased eryptosis in smokers is associated with the antioxidant status and C-reactive protein levels. Toxicology. 2019;411:43–8.
7. Borst O, Abed M, Alesutan I, Towhid ST, Qadri SM, Föller M, et al. Dynamic adhesion of eryptotic erythrocytes to endothelial cells via CXCL16/SR-PSOX. Am J Physiol-Cell Physiol. 2012; 302:C644–51.
8. Walker B, Towhid ST, Schmid E, Hoffmann SM, Abed M, Münzer P, et al. Dynamic adhesion of eryptotic erythrocytes to immobilized platelets via platelet phosphatidylserine receptors. Am J Physiol-Cell Physiol. 2014;306:C291–7.
9. Lang F, Lang KS, Lang PA, Huber SM, Wieder T. Mechanisms and significance of eryptosis. Antioxid Redox Signal. 2006;8(7–8):1183–92.
10. Raducka-Jaszul O, Bogusławska DM, Jedruchniewicz N, Sikorski AF. Role of extrinsic apoptotic signaling pathway during definitive erythropoiesis in normal patients and in patients with β-thalassemia. Int J Mol Sci. 2020;21:3325.
11. Biswas D, Sen G, Sarkar A, Biswas T. Atorvastatin acts synergistically with N-acetyl cysteine to provide therapeutic advantage against Fas-activated erythrocyte apoptosis during chronic arsenic exposure in rats. Toxicol Appl Pharmacol. 2011;250: 39–53.
12. Mandal S, Mukherjee S, Chowdhury KD, Sarkar A, Basu K, Paul S, et al. S-allyl cysteine in combination with clotrimazole downregulates Fas induced apoptotic events in erythrocytes of mice exposed to lead. Biochim Biophys Acta (BBA)-Gen. Subj. 2012;1820:9–23.
13. Restivo I, Attanzio A, Giardina IC, Di Gaudio F, Tesoriere L, Allegra M. Cigarette smoke extract induces p38 MAPK-initiated. Fas-Mediated Eryptosis Int J Mol Sci. 2022;23:14730.
14. Restivo I, Attanzio A, Tesoriere L, Allegra M, Garcia-Llatas G, Cilla A. Anti-eryptotic activity of food-derived phytochemicals and natural compounds. Int J Mol Sci. 2022;23:3019.
15. Attanzio A, Restivo I, Tutone M, Tesoriere L, Allegra M, Livrea MA. Redox properties, bioactivity and health effects of indicaxanthin, a bioavailable phytochemical from Opuntia ficus indica, L.: a critical review of accumulated evidence and perspectives. Antioxidants. 2022;11:2364.
16. Allegra M, D'Acquisto F, Tesoriere L, Attanzio A, Livrea MA. Pro-oxidant activity of indicaxanthin from Opuntia ficus indica modulates arachidonate metabolism and prostaglandin synthesis through lipid peroxide production in LPS-stimulated RAW 264.7 macrophages. Redox Biol. 2014;2:892–900.
17. Allegra M, Ianaro A, Pleurisy CR, Tersigni M, Panza E, Tesoriere L, et al. Indicaxanthin from cactus pear fruit exerts anti-inflammatory effects in carrageenin-induced rat pleurisy. J Nutr. 2014;144(2):185–92.
18. Allegra M, Carletti F, Gambino G, Tutone M, Attanzio A, Tesoriere L, et al. Indicaxanthin from Opuntia ficus-indica crosses the blood-brain barrier and modulates neuronal bioelectric activity in rat hippocampus at dietary-consistent amounts. J Agric Food Chem. 2015;63:7353–60.
19. Allegra M, De Cicco P, Ercolano G, Attanzio A, Busà R, Cirino G, et al. Indicaxanthin from Opuntia Ficus Indica (L. Mill) impairs melanoma cell proliferation, invasiveness, and tumor progression. Phytomedicine. 2018;50:19–24.
20. Tesoriere L, Allegra M, Butera D, Livrea MA. Absorption, excretion, and distribution of dietary antioxidant betalains in LDLs: potential health effects of betalains in humans. Am J Clin Nutr. 2004;80:941–5.

21. Turco Liveri ML, Sciascia L, Allegra M, Tesoriere L, Livrea MA. Partition of Indicaxanthin in membrane biomimetic systems. A kinetic and modeling approach. J Agric Food Chem. 2009;57:10959–63.
22. Tesoriere L, Butera D, Allegra M, Fazzari M, Livrea MA. Distribution of betalain pigments in red blood cells after consumption of cactus pear fruits and increased resistance of the cells to ex vivo induced oxidative hemolysis in humans. J Agric Food Chem. 2005;53:1266–70.
23. Tesoriere L, Attanzio A, Allegra M, Livrea MA. Dietary indicaxanthin from cactus pear (Opuntia ficus-indica L. mill) fruit prevents eryptosis induced by oxysterols in a hypercholesterolaemia relevant proportion and adhesion of human erythrocytes to endothelial cell layers. Br J Nutr. 2015;114:368–75.
24. Tesoriere L, Attanzio A, Allegra M, Gentile C, Livrea MA. Phytochemical indicaxanthin suppresses 7-ketocholesterol-induced THP-1 cell apoptosis by preventing cytosolic $Ca^{2+}$ increase and oxidative stress. Br J Nutr. 2013;110:230–40.
25. Piattelli M, Minale L, Prota G. Isolation structure and absolute configuration of indicaxanthin. Tetrahedron. 1964;20:2325–9.
26. Tesoriere L, Attanzio A, Allegra M, Cilla A, Gentile C, Livrea MA. Oxysterol mixture in hypercholesterolemia-relevant proportion causes oxidative stress-dependent eryptosis. Cell Physiol Biochem. 2014;34:1075–89.
27. Grassmé H, Riethmüller J, Gulbins E. Biological aspects of ceramide-enriched membrane domains. Prog Lipid Res. 2007;46:161–70.
28. Islam F, Roy S, Zehravi M, Paul S, Sutradhar H, Yaidikar L, et al. Polyphenols targeting MAP kinase signaling pathway in neurological diseases: understanding molecular mechanisms and therapeutic targets. Mol Neurobiol. 2023. https://doi.org/10.1007/s12035-023-03706-z
29. Khakh BS, Burnstock G. The double life of ATP. Sci Am. 2009;301:84–90.
30. Arnett DK, Blumenthal RS, Albert MA, Buroker AB, Goldberger ZD, Hahn EJ, et al. ACC/AHA Guideline on the primary prevention of cardiovascular disease: a report of the American College of Cardiology/American Heart Association Task Force on Clinical Practice Guidelines. Circulation. 2019;140(11):e596–646.
31. Closse C, Dachary-Prigent J, Boisseau MR. Phosphatidylserine-related adhesion of human erythrocytes to vascular endothelium. Br J Haematol. 1999;107:300–2.

**How to cite this article:** Restivo I, Giardina IC, Barone R, Cilla A, Burgio S, Allegra M, et al. Indicaxanthin prevents eryptosis induced by cigarette smoke extract by interfering with active Fas-mediated signaling. BioFactors. 2024;50(5):997–1008. https://doi.org/10.1002/biof.2051